CORM-401 induces calcium signalling, NO increase and activation of pentose phosphate pathway in endothelial cells

Patrycja Kaczara[1], Bartosz Proniewski[1], Christopher Lovejoy[2], Kamil Kuś[1], Roberto Motterlini[3], Andrey Y. Abramov[2],* Stefan Chlopicki[1],*

*corresponding authors

[1]Jagiellonian Centre for Experimental Therapeutics (JCET), Jagiellonian University, Krakow 30-348, Poland

[2]Department of Molecular Neuroscience, UCL Institute of Neurology, Queen Square, London WC1N 3BG, UK

[3]INSERM Unit 955, Equipe 12, University Paris-Est, Faculty of Medicine, Créteil, 94000, France

*correspondence:

Prof. Andrey Y. Abramov

Queen Square

London WC1N 3BG

Phone: +442034484062

e-mail: a.abramov@ucl.ac.uk

Prof. Stefan Chlopicki, MD,PhD

Bobrzynskiego, 14

30-348 Krakow, Poland

Phone: +48 126645464

e-mail: stefan.chlopicki@jcet.eu

Running title: CO-induced NO and Ca^{2+} signalling in endothelial cells

Keywords: Endothelium, Carbon Monoxide, Nitric Oxide, Calcium, Ryanodine Receptor, Pentose Phosphate Pathway, NADPH

Article type   : Original Article

Conflicts of interest: None

Abstract

Carbon monoxide-releasing molecules (CO-RMs) induce nitric oxide (NO) release (which requires NADPH), and Ca^{2+}-dependent signalling; however, their contribution in mediating endothelial responses is not clear. Here, we studied the effects of CO liberated from CORM-401 on NO production, calcium signalling and pentose phosphate pathway (PPP) activity in human endothelial cell line (EA.hy926). CORM-401 induced NO production and two types of calcium signalling: a peak-like calcium signal and a gradual increase in cytosolic calcium. CORM-401-induced peak-like calcium signal, originating from endoplasmic reticulum, was reduced by thapsigargin, a SERCA inhibitor, and by dantrolene, a ryanodine receptors (RyR) inhibitor. In contrast, the phospholipase C (PLC) inhibitor U73122 did not significantly affect peak-like calcium signalling, but a slow and progressive CORM-401-induced increase in

cytosolic calcium was dependent on store-operated calcium entrance. CORM-401 augmented coupling of endoplasmic reticulum and plasmalemmal store-operated calcium channels (SOC). Interestingly, in the presence of NO synthase inhibitor (L-NAME) CORM-401-induced increases in NO and cytosolic calcium were both abrogated. CORM-401-induced calcium signalling was also inhibited by superoxide dismutase (PEG-SOD). Furthermore, CORM-401 accelerated PPP, increased NADPH concentration and decreased the ratio of reduced to oxidized glutathione (GSH/GSSG). Importantly, CORM-401-induced NO increase was inhibited by the PPP inhibitor 6-aminonicotinamide (6-AN), but neither by dantrolene nor by an inhibitor of large-conductance calcium-regulated potassium ion channel (paxilline). The results identify the primary role of CO-induced NO increase in the regulation of endothelial calcium signalling, that may have important consequences in controlling endothelial function.

1. Introduction

Carbon monoxide (CO), a product of heme degradation by heme oxygenase enzymes, appears to be an important mediator of vascular function and homeostasis. Different mechanisms of action by CO have been proposed including interaction with various ion channels, activation of soluble guanylate cyclase (sGC), NO release and calcium signalling. Depending on the conditions and the concentrations of CO being used, the mechanisms of action by CO have been shown to exert either beneficial or detrimental effects on specific physiological and biological processes [1]. One of the most extensively studied effects mediated by CO involves interaction with ion channels including large-conductance calcium-regulated potassium ion channels (BK_{Ca}) [2–5], voltage-gated delayed rectifier potassium channels (KV2.1) [6], voltage-gated sodium channels [7] and voltage gated calcium channels (VGCCs) [8]. Although studies reported that CO can increase nitric oxide (NO) production [9–11] and trigger calcium signalling in the endothelium [11,12], the interplay of these two important pathways in endothelial response to CO remains unclear.

We demonstrated recently that CO activates BK_{Ca} channels in mitoplasts derived from endothelial cells, even in the absence of calcium ions [4], suggesting the direct action of CO on mitoBK$_{Ca}$ channels. Although the mitoplast preparation allows to study the activity of ion channels by patch-clamp technique, it is devoid of cellular microenvironments; thus, this preparation does not closely represent the physiological conditions. Interestingly, it was reported that CO-induced vasodilation was mediated by activation of BK_{Ca} channels and effective coupling of Ca^{2+} ions sparks to BK_{Ca} channels [13,14]. Furthermore, some authors suggested that the mechanism of CO-induced vasodilation is independent of the presence of

intact endothelium and mediated by activation of sGC pathway and BK_{Ca} channels [14], while others proposed the involvement of increased endothelial NO generation by CO [9,10]. Given that NO production in endothelial cells is usually activated by Ca^{2+}-dependent mechanisms, and requires NAPDH, which is generated by pentose phosphate pathway (PPP), we wondered whether the effects of CO in endothelial cells are regulated by a link between NO, PPP and calcium signalling.

Calcium signalling plays a fundamental role in endothelial cells by regulating diverse intra- and intercellular biochemical and functional processes, including the production of NO and reactive oxygen species (ROS) as well as cell bioenergetics, motility, angiogenesis, proliferation and regeneration [15–17]. The production of NO may result from Ca^{2+}-mediated signalling initiated by agonist-receptor interaction (e.g. bradykinin, acetylcholine, ATP, VEGF) or mechanical stimuli (flow, shear stress) [17–19]. Several reports have shown that NO- and Ca^{2+}-triggered signals often depend on one another making it difficult to determine which of them is upstream. Furthermore, endothelial nitric oxide synthase (NOS) activity is supported by PPP, as glucose-6-phosphate dehydrogenase (G6PD) and 6-phosphogluconate dehydrogenase (6PGD) represent the major enzymatic sources of NADPH, required for NOS [20], and PPP deficiency leads to impaired NO synthesis [21].

Here we aimed at investigating the mechanisms involved in CO-induced calcium and NO signalling in intact endothelial cells looking also at the possible involvement of PPP.

2. Results

2.1. Effect of CORM-401 on NO production in endothelial cells

Following incubation of endothelial EA.hy926 cells with a donor of carbon monoxide CORM-401 (100 µM, 1h), we found, using EPR spectroscopy, a 5.2-fold increase in NO production compared to untreated cells and 5.7-fold increase compared to cells subjected to inactive CORM-401 (negative control), which does not liberate CO (iCORM-401; Fig. 1A-B). Importantly, pre-incubation of cells with 100 µM L-NAME (20 min), an inhibitor of endothelial NO synthase (NOS), completely abolished CORM-401-induced NO production.

2.2. Effect of CORM-401 on cytosolic calcium concentration in endothelial cells

Addition of CORM-401 (30 µM) to intact EA.hy926 cells induced an elevation in cytosolic calcium ($[Ca^{2+}]_c$), as measured with fura-2 (Fig. 2A) or fluo-4 (Fig. 2B) as indicators using fluorescence microscopy. The pattern of signal was variable (not homogeneous for all cells) and consisted of: a) a slow and gradual increase in $[Ca^{2+}]_c$ (in 25% of cells, n=55, Fig.

2A; in 43% of cells, n=14, Fig. 2B); b) peak-like increases in $[Ca^{2+}]_c$ seen as low amplitude $[Ca^{2+}]_c$ oscillations or fluctuations in combination with the slow and gradual signal (in 75% of cells, n=55 in Fig. 2A, in 57% of cells, n=14 in Fig. 2B; Fig. 2C). iCORM-401 did not affect the levels of cytosolic calcium suggesting that CO directly mediates the observed effect. Neither the slow and gradual increase in $[Ca^{2+}]_c$ nor peak-like increase in $[Ca^{2+}]_c$ was induced by iCORM-401 (Fig. 2D).

2.3. Exploration of potential sources of Ca^{2+} ions influx into the cytoplasm in response to CORM-401 in endothelial cells

In order to identify whether the source of the CO-induced calcium signals in EA.hy926 cells is extracellular or intracellular, we tested the response to CORM-401 (30 µM) in cells incubated in calcium-free medium (Ca^{2+}-free HBSS plus 0.5 mM EGTA). In this experimental setting CORM-401 still induced peak-like increases in $[Ca^{2+}]_c$ (present in 61% of the cells, n=151; Fig. 3A), suggesting that external calcium is not crucial for this type of CO-induced calcium signal; however, the gradual increase in $[Ca^{2+}]_c$ was significantly suppressed.

Recently we found that CORM-401 induced an acceleration of mitochondrial respiration and an increase in oligomycin-insensitive oxygen consumption rate, related to proton leak [4]. The observed effects were diminished after inhibition of BK_{Ca} channel using paxilline. In order to investigate whether BK_{Ca} channel plays a role in CO-induced calcium signalling, we pre-treated cells with paxilline (10 µM, n=40; Fig. 3B) and found that inhibition of BK_{Ca} did not affect calcium signals induced by CORM-401. Considering the role of CO in mitochondrial physiology [22] and the role of mitochondria in the regulation of cytosolic calcium signals, we tested the response to CORM-401 in the presence of a mitochondrial uncoupler (FCCP), which depolarizes mitochondrial membrane, releases mitochondrial Ca^{2+} ions and blocks the further uptake of calcium into the mitochondria. Application of 0.5 µM FCCP did not affect the CO-induced gradual increase in $[Ca^{2+}]_c$ (Fig. 3C; n=158) suggesting that the gradual elevation of intracellular calcium by CO is not released from mitochondria. On the other hand, peak-like increases in $[Ca^{2+}]_c$ were absent. It should be noted that pre-treatment of intact cells with FCCP may diminish calcium mitochondrial buffering capacity and lead to energy deprivation, which can affect active calcium transport [23] and may explain FCCP-dependent changes of CORM-401-induced calcium signals.

In order to verify whether CORM-401-induced $[Ca^{2+}]_c$ signals originate from the endoplasmic reticulum (ER), we added CORM-401 to EA.hy926 cells pre-incubated with 1 µM thapsigargin, an inhibitor of SERCA pumps. This treatment caused a depletion of Ca^{2+}

ions from ER (Fig. 4A, n=150), but did not induce any additional changes in $[Ca^{2+}]_c$. These data strongly suggest that endoplasmic reticulum plays a key role in CORM-401-induced $[Ca^{2+}]_c$ signalling, representing a major source of Ca^{2+} released in response to CO.

2.4. *Role of ryanodine receptors and NO in CORM-401-activated calcium signalling in endothelial cells*

Peak-like $[Ca^{2+}]_c$ signals activated by CORM-401 appeared to be typical for IP_3-mediated $[Ca^{2+}]_c$ release from ER. We therefore considered whether CO acts as a trigger for activation of phospholipase C (PLC), which by generation of IP_3 can mobilize ER to release Ca^{2+}. However, incubation of EA.hy926 cells with U73122 (5µM, Fig. 4B, n=150), an inhibitor of phospholipase C, did not inhibit CORM-401-induced peak-like $[Ca^{2+}]_c$ signals. These data suggest that PLC- and IP_3- mediated signalling does not play a major role in CO-mediated peak-like $[Ca^{2+}]_c$ responses. Similarly, there was no effect of U73122 on the slow and gradual increase in $[Ca^{2+}]_c$. In turn, a 30 min pre-incubation of the EA.hy926 cells with dantrolene (n=67), an inhibitor of ryanodine receptor (RyR), completely blocked the effect of CORM-401 on both types of calcium signals (Fig. 4C). These data suggest that in EA.hy926 cells CO triggers both types of calcium signals coming from ER through the activation of RyR receptors.

The activation of RyR in endothelial cells can be triggered by NO [24] through reversible nitrosylation of its cysteine sulfhydryl groups [25]. As shown in Fig. 5A (n=230), an inhibition of NO synthase with L-NAME (100 µM) completely blocked CO-induced calcium signals (Fig. 5A; n=230) in EA.hy926 cells strongly suggesting a mechanistic role of endogenous NO in triggering activation of RyR upon CORM-401 exposure. It was reported that NO activates RyR indirectly, *via* formation of peroxynitrite from NO interacting with superoxide anion [25,26]. Although the application of CORM-401 to EA.hy926 cells did not seem to increase basal superoxide production [22], a treatment with superoxide dismutase (30 min pre-incubation with 100 U/ml PEG-SOD) completely blocked CO-induced $[Ca^{2+}]_c$ signals (Fig. 5B). However, a peroxynitrite decomposition catalyst FeTPPS (25 µM) did not block CO-induced $[Ca^{2+}]_c$ signals (Fig. 5C). On the other side, the ratio of reduced to oxidized glutathione (GSH/GSSG) was decreased under CORM-401 treatment (Fig. 5D). Thus, NO, produced in response to CO, and basal superoxide anion, seem to be involved in activation of RyR induced by CO liberated from CORM-401, but peroxynitrite is not the key trigger. All the data allow to suspect an involvement of reactive oxygen or nitrogen species and redox regulation in the activation of RyR, however more specific and sensitive techniques are needed to delineate the exact mechanism involved.

2.5. Participation of store-operated calcium entrance in CORM-401-induced gradual $[Ca^{2+}]_c$ increase in endothelial cells

As shown in Fig. 3A, the slow and progressive $[Ca^{2+}]_c$ increase in EA.hy926 cells was dependent on external calcium suggesting a role for plasmalemmal Ca^{2+} ions channels. Considering that ER calcium content, depleted due to CORM-401-induced RyR activation, can be refilled by store-operated calcium (SOC) entrance [27], we designed an experiment in Ca^{2+}-free medium (calcium free HBSS plus 0.5 mM EGTA). As shown in Fig. 6A-B, addition of thapsigargin (1µM) to EA.hy926 cells pre-incubated with CORM-401 depleted calcium pool of ER and induced, *via* SOC entrance after application of Ca^{2+} ions (1.2 mM $CaCl_2$) to the medium, a significant increase in $[Ca^{2+}]_c$ by 2-fold as compared to untreated (control) or cells stimulated with iCORM-401 (Fig. 6A-C; n=167 for control; n=278 for iCORM-401). Thus, a slow and progressive $[Ca^{2+}]_c$ increase in response to CO was stimulated by the activation of SOC entrance. Accordingly, CO seems to enhance the coupling between ER content and SOC entrance into the endothelium.

2.6. Exploration of potential triggers for CORM-401-induced NO increase in endothelial cells

We demonstrated previously that CO activates mitochondrial BK_{Ca} channels and this effect was inhibited by paxilline [4]. Since it was demonstrated by others that an activation of BK_{Ca} channels results in NO release and vasodilation [28], we analysed the involvement of BK_{Ca} channels in CO-induced NO increase in the endothelium. As shown in Fig. 7A, paxilline (10 µM) did not affect CO-induced NO production in endothelial cells. NO production was also not affected by dantrolene nor U73122 (Fig.7A), suggesting that CO-induced NO production is not mediated by the activation of RyR or PLC.

NO synthesis by endothelial nitric oxide synthase (eNOS) requires electrons from NADPH [20,21] and two enzymes of PPP, glucose-6-pfhosphate dehydrogenase (G6PD) and 6-phosphogluconate dehydrogenase (6PGD), which represent the major enzymatic source of NADPH. Analysis of intracellular metabolites was performed using targeted mass spectrometry-based metabolomics. As shown in Fig. 8A, CORM-401 induced a significant increase in NADPH concentration, enabling enhanced production of NO, while inhibition of PPP with 6-aminonicotinamide (200 µM, 4h of pre-incubation; 6-AN, an inhibitor of 6-phosphogluconate dehydrogenase) completely reduced NADPH concentration and significantly diminished CO-induced NO production in endothelial cells (Fig. 7B). Still, basal NO production in non-stimulated cells was not changed under treatment with 6-AN, suggesting that the activation of PPP by CO may be required for augmented production of NO, whereas basal NO release may occur without additional activation of PPP. To further

confirm that CO activates PPP, we measured the levels of intracellular metabolites of PPP and demonstrated that CORM-401 indeed increased the ratio of ribulose-5-phosphate (R5P) to its precursor 6-phosphogluconate (6PG), as compared to untreated control (Fig. 8B), indicating acceleration of PPP. Activation of PPP by CORM-401 was not observed in cells pre-incubated with 6-AN, while the R5P/6PG ratio was substantially decreased (Fig. 8B); 6-AN efficiently inhibited 6-phosphogluconate dehydrogenase, what was additionally evidenced by highly increased intracellular concentration of 6-phosphogluconate (Fig. 8C). Moreover, CORM-401 increased also the concentration of intracellular metabolites of PPP such as erythrose 4-phosphate (152 ± 28%), pentoses 5-phosphates (ribulose –phosphate, xylulose 5-phosphate and ribose 5-phosphate, 119 ± 26%), and sedoheptulose 7-phosphate (126 ± 14%), compatible with the activation of PPP.

3. Discussion

Here we demonstrate that in the endothelium-derived cell line CO induces NO release, which is supported by NAPDH from the pentose phosphate pathway (PPP), and regulates calcium signalling. Even though there are several articles reporting on the different signalling pathways that are controlled by calcium, CO and NO [2,8–10,12–14,18,24,26], our results extend and point to the implication of PPP in NO increase and calcium signalling induced by CO in the endothelium, which may have an important role in the regulation of endothelial phenotypes. Furthermore, our results identify a major role of RyR receptors and redox signalling, involving NO/superoxide or other ROS, in CORM-401-induced increase in $[Ca^{2+}]_c$, as well as a coupling between ER content and store-operated Ca^{2+} channel (SOC) entrance in mediating CORM-401-induced $[Ca^{2+}]_c$ response. Altogether, our results demonstrate that the complex interlinked signalling of CO in endothelial cells involves NO production, activation of PPP and calcium signalling.

3.1. CO-induced NO production in the endothelium

In the present work we clearly demonstrate that CO liberated from CORM-401 induces NO production in endothelial cells. Similar effects have been described for other CO-RMs or CO gas in different cell types or vascular tissue preparations [9–12,29]. Various mechanisms responsible for NO increase following CO treatment were proposed previously; they include displacement of NO from a cellular storage pool [9] or activation of NO synthase *via* calcium or phosphatidylinositol 3-kinase/Akt pathways [11,12,29]. In our hands CO-induced NO increase in endothelial cells is completely blocked by L-NAME, confirming that NO is indeed produced by eNOS and not released from a cellular storage pool (Fig. 1). Complex mechanisms of eNOS activation (for review see [30,31]) allow to consider several possible triggers for CO-induced NO production, involving (1) phosphatidylinositol 3-kinase-

serine-theronine kinase Akt/protein kinase B - NOS (IP3K-Akt/PKB-NOS) pathway, and (2) Ca^{2+}/calmodulin (CaM)-mediated NOS activation [11,12,29]. As the inhibition of ER calcium channels did not affect NO release in our experimental setting (Fig. 7A), we conclude that Ca^{2+}/CaM-dependent mechanism was not a primary pathway involved in CO-induced NO production, although it could contribute at the latter stage of stimulation, e. g. after accumulation of Ca^{2+} ions in cytoplasm followed by CO-induced gradual Ca^{2+} ions increase. We did not study the involvement of IP3K-Akt/PKB-NOS that was previously reported to mediate CO-induced NO production [11]. However, we demonstrated that CO-induced NO increase in endothelial cells was supported by the activation of PPP, as evidenced by substantial increase in NAPDH cytosolic concentration accompanied by increased concentrations of PPP metabolites in response to CORM-401 (Fig. 8). Furthermore, the inhibitory effects of 6-aminonicotinamide (6-AN, an inhibitor of 6-phosphogluconate dehydrogenase) on CORM-401-induced NO increase (Fig. 7B) clearly indicate a role of PPP in CO-induced NO production. The inhibition of PPP by 6-AN was evidenced by increased intracellular concentration of 6-phosphogluconate in line with the inhibition of PPP at the level of 6-phosphogluconate dehydrogenase. The activation of PPP by CO are in agreement with a previous report showing that CORM-2, a ruthenium-based CO-releasing agent, induces a shift of glucose biotransformation towards an increase in PPP metabolites in leukemia cell line [32].

Although it was previously demonstrated that CORM-401 inhibits glycolysis [4,22] and shunts glucose to PPP [32], the functional role of PPP in endothelial cells in response to CO has not been previously appreciated. In particular, although it was demonstrated that overexpression of glucose-6-phosphate dehydrogenase (G6PD) in bovine aortic endothelial cells results in an increased NO production [21], while G6PD deficiency is associated with a decrease in NO availability [33], in the present work NO increase induced by CO was mechanistically linked to the PPP activation for the first time. G6PD and 6-phosphogluconate dehydrogenase (6PGD), the first rate-limiting and the third enzymes in PPP, represent the enzymatic sources of NADPH, which is an important electron donor for endothelial NO synthase (NOS) [20]. Another source of NADPH could be isocitrite dehydrogenase, however the reason why we decided not to perform another experiments with inhibition of citrate dehydrogenase is that we obtained a very deep decrease in NADPH concentration after the inhibition of PPP with 6-AN (Fig. 8A), confirming the importance of G6PD and 6PGD in NADPH production in our model. Indeed, during the synthesis of NO, NADPH-derived electrons are required for heme iron to bind oxygen and catalyse the stepwise synthesis of NO from L-arginine [30]. CO-induced activation of PPP may thus increase the availability of NADPH that is used by NOS to produce NO.

On the other hand, we exclude in the present work the involvement of large-conductance calcium regulated potassium ion channels (BK_{Ca}) in CO-mediated NO increase, as its inhibitor – paxilline - did not block CORM-401-induced NO increase in endothelial cells. This is in contrast to the work of Jaggar *et al.* [13], who demonstrated an involvement of BK_{Ca} channels in vasodilation induced by CO in cerebral vascular smooth muscle cells. However, this discrepancy may result from different experimental models used. Yet, the endothelium shows remarkable heterogeneity in terms of function, structure and phenotype, which depend on the microenvironment and the vascular bed of origin, as well as health and disease [34].

We demonstrated previously that CORM-401 activates BK_{Ca} channels in intact endothelial cells (resulting in increased basal respiration, proton leak and mild uncoupling), but also directly in mitoplasts devoid of intracellular milieu and cytosolic calcium [4]. However, in the context of present data we speculate that the effects observed previously in intact cells resulted from activation of BK_{Ca} channels by calcium signals rather than from their direct activation by CO. Interestingly, Jaggar et al. [13] demonstrated that CO dilates cerebral arterioles by enhancing the coupling of Ca^{2+} sparks to BK_{Ca} channels in smooth muscle cells. Moreover, potassium influx by $mitoBK_{Ca}$ channels can increase a volume of mitochondrial matrix [35], followed by an increase in mitochondrial respiration, which can also result from diverse mechanisms dependent on calcium signalling, such as activation of ATP-consuming processes, activation of pyruvate dehydrogenase and other mitochondrial dehydrogenases that deliver NADH to electron transport chain [36].

3.2. *CO-induced calcium and redox signalling in the endothelium*

In the present work we demonstrate that slow/gradual and peak-like Ca^{2+} signals, both induced by CO, are blocked by dantrolene, an inhibitor of RyR. Accordingly, CO-induced calcium signalling is initiated by the opening of RyR channels in the ER. Moreover, slow/gradual calcium increase was completely blocked also in Ca^{2+}–free buffer (Fig. 3), strongly suggesting that slow calcium elevation in cytosol is induced by specific activation of SOC. Other plasmalemmal channels or the purinergic cascade, which involves activation of phospholipase C (PLC) [37], seem to play rather a minor role in slow calcium release [38]; accordingly, in our experiments inhibition of PLC only slightly weaken CO-induced calcium signals. Furthermore, in the presence of CORM-401 and the blockade of sarco/endoplasmic reticulum Ca^{2+}-ATPases (SERCA), the effect of extracellular calcium on intracellular calcium rise was potentiated suggesting that CO augments coupling of RyR channels in ER and activates plasmalemmal SOC. However, the mechanisms involved in this regulation are not entirely clear. RyR does not contain any direct targets for CO, as heme or Fe-S centres,

though RyR can be activated by redox mechanisms involving oxidation of sufhydryl groups in cysteine residues [25,26]. We demonstrate here that inhibition of NO production by L-NAME or inhibition of superoxide production by PEG-SOD completely blocked CO-induced calcium signalling, suggesting the involvement of peroxynitrite. Interestingly, we demonstrated previously that CORM-401 did not increase superoxide generation in EA.hy926 cells [22], implicating that increased NO and basal superoxide were involved in RyR activation. This could stay in line with the results showing NO-triggered Ca^{2+} ions release from ER in rat hippocampal neurons, mediated by both IP3R1 and RyR, which required physiological ROS levels only [39]. Although in the present work we demonstrate that CO-induced calcium signalling is dependent on NO and augments coupling of RyR channels in ER with plasmalemmal SOC, we cannot exclude IP_3-dependent or other mechanisms.

The role of CO in the modulation of ROS signaling is an important, but ambiguous issue. A number of reports show an increased ROS generation following an exposure of cells or tissues to CO [40–44]. It is speculated that CO stimulates mitochondria by the partial inhibition of cytochrome c oxidase, leading to generation of low amounts of ROS that are important signalling molecules (for review see [45]). On the other side, we demonstrated previously [4,22,42,46] that CO uncouples mitochondria and reduces mitochondrial membrane potential in EA.hy926 cells, what can play a protective role against oxidative stress. Moreover, in the present work we observe a decreased ratio of reduced to oxidized glutathione (GSH/GSSG) following CO exposure (Fig. 8C), what can result from utilization of GSH to neutralize ROS generated in response to CO. Simultaneously, CO-induced activation of PPP and subsequently increased production of NADPH (Fig. 8A) seem also be important to restore a reduced pool of GSH *via* glutathione reductase, which converts GSSG to GSH to maintain intercellular stores of reduced glutathione (GSH), essential to neutralize ROS. Previously we did not observe in endothelial cells increased ROS production in response to CO [22], but it did not mean that they were not produced. It might well be that ROS were not detected or undergo rapid neutralization. Interestingly, it was demonstrated by others that CO by the enhancement of the ratio of oxidized to reduced glutathione (GSSG/GSH) induces glutathionylation of adenine nucleotide translocase (ANT) in astrocytes, protecting the cells from apoptosis [47] and glutathionylation of p65 in endothelial cells, leading to anti-inflammatory effects [48]. Thus, CO-induced redox regulation may involve also glutathionylation, which may result in cytoprotective effects [45]. Altogether, CO-induced redox signalling, involving NO, ROS, glutathione and RyR-dependent calcium signalling, may be well balanced by the activation of cytoprotective mechanisms well demonstrated for the activation of PPP in various experimental set-ups [20].

In addition, activation of PPP may be also involved *per se* in redox-controlled regulation of Ca^{2+} ions homeostasis, as the inhibition of this pathway in vascular cells reduces intracellular Ca^{2+} ions concentration by blocking its release [49]. On the other hand, inhibition of G6PD in cardiomyocytes impairs their contractility through dysregulation of Ca^{2+} ions homeostasis [50]. Apparently, the activation of PPP may represent an important regulatory mechanism linking CO with calcium signalling.

In conclusion, we demonstrate here that CO induces an increased production of NO triggering calcium signalling, as well as augments coupling of endoplasmic reticulum with plasmalemmal SOC in endothelial cells. Increased NO production is supported by the activation of pentose phosphate pathway, an important cytoprotective pathway, whereas activation of calcium signalling is dependent on NO, redox signalling and activation of ryanodine receptors. Thus, CO at low concentrations appears to play a role as a fine regulator in intracellular signalling system, which may have consequences in the regulation of complex and interrelated mechanisms that protect vascular endothelial cells.

4. Materials and methods

4.1. Reagents

CORM-401, a Mn-containing water-soluble CO-releasing molecule releasing at least three moles of CO molecules per one mole of the compound (half-life of 13-14 min), was used to deliver CO [4,22,46,51]. Inactive CORM-401 (iCORM-401; contains $MnSO_4$ and the ligand for CORM-401), which does not liberate CO, was used to exclude the effects of other than CO components of the moiety. Dulbecco's Modified Eagle Medium (DMEM), fetal bovine serum (FBS), HAT supplement, penicillin/streptomycin, and trypsin were obtained from Gibco-Invitrogen, Paisley, UK. 6-aminonicotinamide (6-AN), carbonyl cyanide 4-(trifluoromethoxy)phenylhydrazone (FCCP), $MnSO_4$, ethylene glycol-bis(2-aminoethylether)-N,N,N′,N′-tetraacetic acid (EGTA), Nω-Nitro-L-arginine methyl ester hydrochloride (L-NAME), NaCl, KCl, $MgSO_4$, KH_2PO_4, $CaCl_2$, glucose, 4-(2-Hydroxyethyl)piperazine-1-ethanesulfonic acid (HEPES), NaOH, $FeSO_4 \times 7H_2O$, superoxide dismutase–polyethylene glycol (PEG-SOD), were obtained from Sigma-Aldrich, St. Louis, MO, USA. Fluorescent dyes: Fura-2, Fluo-4 and Pluronic were obtained from Invitrogen, Paisley, UK. Thapsigargin, U73122, paxilline and dantrolene were obtained from Tocris Bioscience, Bristol, UK. Diethylthiocarbonic acid (DETC) was obtained from Enzo Life Sciences Inc., Farmingdale, NY, USA. FeTPPS was obtained from Cayman Chemical Company, Michigan, USA. CORM-401 was synthesized as described previously [51]. All live cell imaging experiments were performed by using 30 µM CORM-401, a concentration selected from our previous work [4] showing that the release of CO from this compound induced a slight acceleration of oxygen

consumption rate in EA.hy926 cells. Due to methodological limitations (reduced ratio of buffer volume to number of cells) all experiments for analysis of NO production by EA.hy926 were performed using 100 µM CORM-401, thus the ratio between moles of CORM-401 molecules and the number of cells were comparable in two different experimental setups.

4.2. Cell culture

The hybridoma endothelial EA.hy926 cell line, formed by fusion of human umbilical vein endothelial cells (HUVEC) with the A549 human lung carcinoma cell line, was kindly provided by Dr. C-J Edgell (Department of Pathology, University of North Carolina, Chapel Hill, NC, USA) [52]. Cells were propagated using three weekly feedings of DMEM containing 10% FBS, 1 g l^{-1} glucose, 110 mg l^{-1} sodium pyruvate, 2 mM GlutaMAX™, antibiotics (100 IU penicillin, 100 µg ml^{-1} streptomycin) and 2% HAT Supplement. Cultures were maintained at 37 °C in a fully humidified atmosphere of 5% CO_2 in air. Cells were confirmed to be contamination-free. For live cell imaging, cells were plated into 25 mm coverslips in six-well plates, to get a density of 80-100%.

4.3. Imaging of calcium signalling

Cells were loaded for 30 min at room temperature with 5 µM fura-2 AM or fluo-4 AM and 0.005% Pluronic in a HEPES-buffered salt solution (HBSS) composed (mM): 156 NaCl, 3 KCl, 2MgSO$_4$, 1.25 KH$_2$PO$_4$, 2 CaCl$_2$, 10 glucose and 10 HEPES, pH adjusted to 7.35 with NaOH. Ca^{2+}-free medium contained 0.5 mM EGTA. Fluorescence measurements were obtained on an epifluorescence inverted microscope equipped with a 20x fluorite objective. Cytosolic calcium concentration ($[Ca^{2+}]_c$) was monitored in single cells using excitation light provided by a Xenon arc lamp, the beam passing monochromator at 340 and 380 nm (Cairn Research, Kent, UK). Emitted fluorescence light was reflected through a 515 nm long-pass filter to a cooled CCD camera (Retiga, QImaging, Canada) and digitised to 12 bit resolution. All imaging data were collected and analysed using software from Andor (Belfast, UK). The fura-2 data have not been calibrated in terms of $[Ca^{2+}]_c$ because of the uncertainty arising from the use of different calibration techniques.

Confocal images were obtained using a Zeiss 710 CLSM system and a 40x oil immersion objective. The 488nm Argon laser line was used to excite fluo-4 which was measured at 505-550 nm. Illumination intensity was kept to a minimum (at 0.1-0.2% of laser output) to avoid phototoxicity and the pinhole set to give an optical slice of ~2µm.

4.4. Analysis of NO production by endothelial cells

Colloidal $Fe^{2+}(DETC)_2$ was used for trapping intracellular NO with electron paramagnetic resonance (EPR) detection as described previously with minor modifications [53]. Briefly, EA.hy926 cells were plated on 60 mm Petri dishes to achieve a confluence.

Saline (0.9% NaCl) was bubbled for 30 min with argon gas on ice to remove oxygen. Culture medium was aspired and 0.6 ml of plain DMEM was added per dish. 2.3 mg of $FeSO_4 x7H_2O$/10 ml for 0.8 mM stock and 3.6 mg of DETC/10 ml for 1.6 mM stock were dissolved separately in bubbled with argon saline, mixed and immediately added to culture dishes with cells (0.2 ml per dish) followed by addition 100 µM CORM-401 or iCORM-401. The cells were incubated for 1 h at 37 ℃, 5% CO2, followed by discarding the medium containing the spin trap, collection of the cells by scraping into 1-ml insulin syringe (200 µl per sample) and snap freezing in liquid nitrogen. Measurement of $NO-Fe^{2+}(DETC)_2$ signal in frozen samples was performed in a finger dewar using EMX Plus Bruker spectrometer with the following settings: microwave power, 10 mW; modulation amplitude, 0.8 mT; scan width, 11.5 mT; scan time, 61.44 s; number of scans, 4. The results were collected and analysed with Processing WinEPR software. The $NO-Fe^{2+}(DETC)_2$ signal was a clear triple-centred at g=2.039 and was quantified as an amplitude of the signal (Fig. 1).

4.5. Analysis of intracellular metabolites

Detection of intracellular metabolites was performed according to the protocol described previously [54] with minor changes. Briefly, confluent EA.hy926 cells (plated in a number of 3×10^6 cells into 100 mm dishes one day before the experiment) were pre-incubated for 4 h with 6-AN (200 µM) or DMSO in complete medium followed by washing and adding plain medium DMEM (with 2 mM GlutaMAX, 5 mM glucose, 1 mM sodium pyruvate) containing DMSO/6-AN (200 µM) and PBS/CORM-401 (100 µM). After 1h incubation, the medium was removed and cells were washed with ice-cold PBS, followed by ice-cold water. Intracellular metabolites were extracted with 2 mL of dry-ice-cold extraction solution (acetonitrile: methanol: water 5:2:3, v/v/v), lyophilized and reconstituted in water. Samples were injected into LC column and analysed on QTRAP 5500 (Sciex, Framingham, MA, USA) coupled to UFLC Nexera (Shimadzu, Kyoto, Japan). Chromatography separation was achieved on Acquity UPLC BEH C18 1.7 µm 3.0 x 100 mm analytical column (Waters, Milford, MA, USA). Samples were analysed twice in positive and negative ionization MRM mode. For the analysis in positive ionisation, acetonitrile and 5 mM ammonium acetate (pH 5.8) were used as a mobile phase in a run time of 8 min. For the analysis in negative ionisation, ACN: 50 mM ammonium acetate (pH 5.8) 90:10 v/v and 5 mM ammonium acetate (pH 5.8) were used as a mobile phase in a run time of 6.5 min.

4.6. Statistical analysis

Statistical analysis was performed using a OriginPro 9.1 software (OriginLab Corporation, Northampton, MA, USA). Results were expressed as means ± SEM. For statistical analysis, one-way ANOVA was performed, *P* values provided in the legends.

Acknowledgments

Author contributions

Study design (PK, AYA, SCH), providing experimental tools (AYA, RM, PK, SCH), study execution (PK, AYA, CL, BP, KK), interpretation of findings (all co-authors), drafting the manuscript (PK, SCH, AYA), revising the manuscript (PK, RM, AYA, SCH).

References

1 Peers C, Boyle JP, Scragg JL, Dallas ML, Al-Owais MM, Hettiarachichi NT, Elies J, Johnson E, Gamper N & Steele DS (2015) Diverse mechanisms underlying the regulation of ion channels by carbon monoxide. *Br. J. Pharmacol.* **172**, 1546–1556.

2 Dong D-L, Zhang Y, Lin D-H, Chen J, Patschan S, Goligorsky MS, Nasjletti A, Yang B-F & Wang W-H (2007) Carbon Monoxide Stimulates the Ca2(+)-Activated Big Conductance K Channels in Cultured Human Endothelial Cells. *Hypertension* **50**, 643–51.

3 Jaggar JH, Li A, Parfenova H, Liu J, Umstot ES, Dopico AM & Leffler CW (2005) Heme Is a Carbon Monoxide Receptor for Large-Conductance Ca2+-Activated K+ Channels. *Circ. Res.* **97**, 805–12.

4 Kaczara P, Motterlini R, Rosen GM, Augustynek B, Bednarczyk P, Szewczyk A, Foresti R & Chlopicki S (2015) Carbon monoxide released by CORM-401 uncouples mitochondrial respiration and inhibits glycolysis in endothelial cells: A role for mitoBKCa channels. *Biochim. Biophys. Acta* **1847**, 1297–1309.

5 Riddle MA & Walker BR (2012) Regulation of endothelial BK channels by heme oxygenase-derived carbon monoxide and caveolin-1. *Am. J. Physiol. Cell Physiol.* **303**, C92–C101.

6 Dallas ML, Boyle JP, Milligan CJ, Sayer R, Kerrigan TL, McKinstry C, Lu P, Mankouri J, Harris M, Scragg JL, Pearson HA & Peers C (2011) Carbon monoxide protects against oxidant-induced apoptosis via inhibition of Kv2.1. *FASEB J.* **25**, 1519–30.

7 Althaus M, Fronius M, Buchäckert Y, Vadász I, Clauss WG, Seeger W, Motterlini R & Morty RE (2009) Carbon monoxide rapidly impairs alveolar fluid clearance by inhibiting epithelial sodium channels. *Am. J. Respir. Cell Mol. Biol.* **41**, 639–50.

8 Lim I, Gibbons SJ, Lyford GL, Miller SM, Strege PR, Sarr MG, Chatterjee S, Szurszewski JH, Shah VH & Farrugia G (2005) Carbon monoxide activates human intestinal smooth muscle L-type Ca2+ channels through a nitric oxide-dependent mechanism. *Am. J. Physiol. Gastrointest. Liver Physiol.* **288**, G7-14.

9 Thorup C, Jones CL, Gross SS, Moore LC & Goligorsky MS (1999) Carbon monoxide induces vasodilation and nitric oxide release but suppresses endothelial NOS. *Am. J. Physiol.* **277**, F882-9.

10 Alshehri A, Bourguignon M-P, Clavreul N, Badier-Commander C, Gosgnach W, Simonet S, Vayssettes-Courchay C, Cordi A, Fabiani J-N, Verbeuren TJ & Félétou M (2013) Mechanisms of the vasorelaxing effects of CORM-3, a water-soluble carbon monoxide-releasing molecule: interactions with eNOS. *Naunyn. Schmiedebergs. Arch. Pharmacol.* **386**, 185–96.

11 Yang P-M, Huang Y-T, Zhang Y-Q, Hsieh C-W & Wung B-S (2016) Carbon monoxide releasing molecule induces endothelial nitric oxide synthase activation through a calcium and phosphatidylinositol 3-kinase/Akt mechanism. *Vascul. Pharmacol.* **87**, 209–218.

12 Moustafa A & Habara Y (2014) A novel role for carbon monoxide as a potent regulator of intracellular Ca2+ and nitric oxide in rat pancreatic acinar cells. *Am. J. Physiol. Cell Physiol.* **307**, C1039-49.

13 Jaggar JH, Leffler CW, Cheranov SY, Tcheranova D, E S & Cheng X (2002) Carbon monoxide dilates cerebral arterioles by enhancing the coupling of Ca2+ sparks to Ca2+-activated K+ channels. *Circ. Res.* **91**, 610–7.

14 Wang R, Wang Z & Wu L (1997) Carbon monoxide-induced vasorelaxation and the underlying mechanisms. *Br. J. Pharmacol.* **121**, 927–34.

15 Munaron L & Scianna M (2012) Multilevel complexity of calcium signaling: Modeling angiogenesis. *World J. Biol. Chem.* **3**, 121–126.

16 Moccia F, Tanzi F & Munaron L (2014) Endothelial remodelling and intracellular calcium machinery. *Curr. Mol. Med.* **14**, 457–80.

17 Tran Q-K, Ohashi K & Watanabe H (2000) Calcium signalling in endothelial cells. *Cardiovasc. Res.* **48**.

18 Sandow SL, Senadheera S, Grayson TH, Welsh DG & Murphy T V (2012) Calcium and endothelium-mediated vasodilator signaling. *Adv. Exp. Med. Biol.* **740**, 811–31.

19 Félétou M (2011) *The Endothelium* Morgan & Claypool Life Sciences.

20 Stanton RC (2012) Glucose-6-phosphate dehydrogenase, NADPH, and cell survival. *IUBMB Life* **64**, 362–369.

21 Leopold JA, Zhang Y-Y, Scribner AW, Stanton RC & Loscalzo J (2003) Glucose-6-phosphate dehydrogenase overexpression decreases endothelial cell oxidant stress and increases bioavailable nitric oxide. *Arterioscler. Thromb. Vasc. Biol.* **23**, 411–7.

22 Kaczara P, Motterlini R, Zakrzewska A, Kuś K, Abramov AY & Chłopicki S (2016) Carbon monoxide shifts energetic metabolism from glycolysis to oxidative phosphorylation in endothelial cells. *FEBS Lett.* **590**, 3469–3480.

23 Abramov AY & Duchen MR (2010) Impaired mitochondrial bioenergetics determines glutamate-induced delayed calcium deregulation in neurons. *Biochim. Biophys. Acta* **1800**, 297–304.

24 Kakizawa S, Yamazawa T & Iino M (2013) Nitric oxide-induced calcium release: activation of type 1 ryanodine receptor by endogenous nitric oxide. *Channels (Austin).* **7**, 1–5.

25 Lanner JT, Georgiou DK, Joshi AD & Hamilton SL (2010) Ryanodine receptors: structure, expression, molecular details, and function in calcium release. *Cold Spring Harb. Perspect. Biol.* **2**, a003996.

26 Xu L, Eu JP, Meissner G & Stamler JS (1998) Activation of the cardiac calcium release channel (ryanodine receptor) by poly-S-nitrosylation. *Science* **279**, 234–7.

27 Cioffi DL & Stevens T (2006) Regulation of endothelial cell barrier function by store-operated calcium entry. *Microcirculation* **13**, 709–23.

28 Vang A, Mazer J, Casserly B & Choudhary G (2010) Activation of endothelial BKCa channels causes pulmonary vasodilation. *Vascul. Pharmacol.* **53**, 122–9.

29 Wegiel B, Gallo DJ, Raman KG, Karlsson JM, Ozanich B, Chin BY, Tzeng E, Ahmad S, Ahmed A, Baty CJ & Otterbein LE (2010) Nitric oxide-dependent bone marrow

progenitor mobilization by carbon monoxide enhances endothelial repair after vascular injury. *Circulation* **121**, 537–48.

30 Forstermann U & Sessa WC (2012) Nitric oxide synthases: regulation and function. *Eur. Heart J.* **33**, 829–837.

31 Fleming I (2010) Molecular mechanisms underlying the activation of eNOS. *Pflügers Arch. - Eur. J. Physiol.* **459**, 793–806.

32 Takano N, Yamamoto T, Adachi T & Suematsu M (2010) Assessing a Shift of Glucose Biotransformation by LC-MS/MS-based Metabolome Analysis in Carbon Monoxide-Exposed Cells. In *Advances in Experimental Medicine and Biology* pp. 101–107.

33 Leopold JA, Cap A, Scribner AW, Stanton RC & Loscalzo J (2001) Glucose-6-phosphate dehydrogenase deficiency promotes endothelial oxidant stress and decreases endothelial nitric oxide bioavailability. *FASEB J.* **15**, 1771–3.

34 Aird WC (2012) Endothelial cell heterogeneity. *Cold Spring Harb. Perspect. Med.* **2**, a006429.

35 O'Rourke B, Cortassa S & Aon MA (2005) Mitochondrial ion channels: gatekeepers of life and death. *Physiology (Bethesda).* **20**, 303–15.

36 Pober JS, Min W & Bradley JR (2009) Mechanisms of endothelial dysfunction, injury, and death. *Annu. Rev. Pathol.* **4**, 71–95.

37 Holmström KM, Marina N, Baev AY, Wood NW, Gourine A V & Abramov AY (2013) Signalling properties of inorganic polyphosphate in the mammalian brain. *Nat. Commun.* **4**, 1362.

38 Nilius B & Droogmans G (2001) Ion channels and their functional role in vascular endothelium. *Physiol. Rev.* **81**, 1415–59.

39 Wilson C, Munoz-Palma E, Henriquez DR, Palmisano I, Nunez MT, Di Giovanni S & Gonzalez-Billault C (2016) A Feed-Forward Mechanism Involving the NOX Complex and RyR-Mediated Ca2+ Release During Axonal Specification. *J. Neurosci.* **36**, 11107–11119.

40 Choi YK, Por ED, Kwon Y-G & Kim Y-M (2012) Regulation of ROS production and vascular function by carbon monoxide. *Oxid. Med. Cell. Longev.* **2012**, 794237.

41 Lancel S, Hassoun SM, Favory R, Decoster B, Motterlini R & Neviere R (2009) Carbon

monoxide rescues mice from lethal sepsis by supporting mitochondrial energetic metabolism and activating mitochondrial biogenesis. *J. Pharmacol. Exp. Ther.* **329**, 641–648.

42 Lo Iacono L, Boczkowski J, Zini R, Salouage I, Berdeaux A, Motterlini R & Morin D (2011) A carbon monoxide-releasing molecule (CORM-3) uncouples mitochondrial respiration and modulates the production of reactive oxygen species. *Free Radic. Biol. Med.* **50**, 1556–64.

43 Zuckerbraun BS, Chin BY, Bilban M, D'Avila JDC, Rao J, Billiar TR & Otterbein LE (2007) Carbon monoxide signals via inhibition of cytochrome c oxidase and generation of mitochondrial reactive oxygen species. *FASEB J.* **21**, 1099–106.

44 Wegiel B, Gallo D, Csizmadia E, Harris C, Belcher J, Vercellotti GM, Penacho N, Seth P, Sukhatme V, Ahmed A, Pandolfi PP, Helczynski L, Bjartell A, Persson JL & Otterbein LE (2013) Carbon monoxide expedites metabolic exhaustion to inhibit tumor growth. *Cancer Res.* **73**, 7009–21.

45 Almeida AS, Figueiredo-Pereira C & Vieira HLA (2015) Carbon monoxide and mitochondriaâ "modulation of cell metabolism, redox response and cell death. *Front. Physiol.* **6**, 33.

46 Wilson JL, Bouillaud F, Almeida AS, Vieira HL, Ouidja MO, Dubois-Randé J-L, Foresti R & Motterlini R (2017) Carbon monoxide reverses the metabolic adaptation of microglia cells to an inflammatory stimulus. *Free Radic. Biol. Med.* **104**, 311–323.

47 Queiroga CSF, Almeida AS, Martel C, Brenner C, Alves PM & Vieira HLA (2010) Glutathionylation of adenine nucleotide translocase induced by carbon monoxide prevents mitochondrial membrane permeabilization and apoptosis. *J. Biol. Chem.* **285**, 17077–88.

48 Yeh P-Y, Li C-Y, Hsieh C-W, Yang Y-C, Yang P-M & Wung B-S (2014) CO-releasing molecules and increased heme oxygenase-1 induce protein S-glutathionylation to modulate NF-κB activity in endothelial cells. *Free Radic. Biol. Med.* **70**, 1–13.

49 Gupte SA, Arshad M, Viola S, Kaminski PM, Ungvari Z, Rabbani G, Koller A & Wolin MS (2003) Pentose phosphate pathway coordinates multiple redox-controlled relaxing mechanisms in bovine coronary arteries. *Am. J. Physiol. - Hear. Circ. Physiol.* **285**, H2316–H2326.

50 Jain M, Brenner DA, Cui L, Lim CC, Wang B, Pimentel DR, Koh S, Sawyer DB, Leopold

JA, Handy DE, Loscalzo J, Apstein CS & Liao R (2003) Glucose-6-Phosphate Dehydrogenase Modulates Cytosolic Redox Status and Contractile Phenotype in Adult Cardiomyocytes. *Circ. Res.* **93**.

51 Crook SH, Mann BE, Meijer AJHM, Adams H, Sawle P, Scapens D & Motterlini R (2011) [Mn(CO)4{S2CNMe(CH2CO2H)}], a new water-soluble CO-releasing molecule. *Dalt. Trans.* **40**, 4230–5.

52 Edgell C, McDonald C & Graham J (1983) Permanent cell line expressing human factor VIII-related antigen established by hybridization. *Proc. Natl. Acad. Sci. U. S. A.* **80**, 3734–7.

53 Cai H, Dikalov S, Griendling K & Harrison D (2007) Detection of Reactive Oxygen Species and Nitric Oxide in Vascular Cells and Tissues. *Vasc. Biol. Protoc.* **139**.

54 Yuan M, Breitkopf SB, Yang X & Asara JM (2012) A positive/negative ion-switching, targeted mass spectrometry-based metabolomics platform for bodily fluids, cells, and fresh and fixed tissue. *Nat. Protoc.* **7**, 872–81.
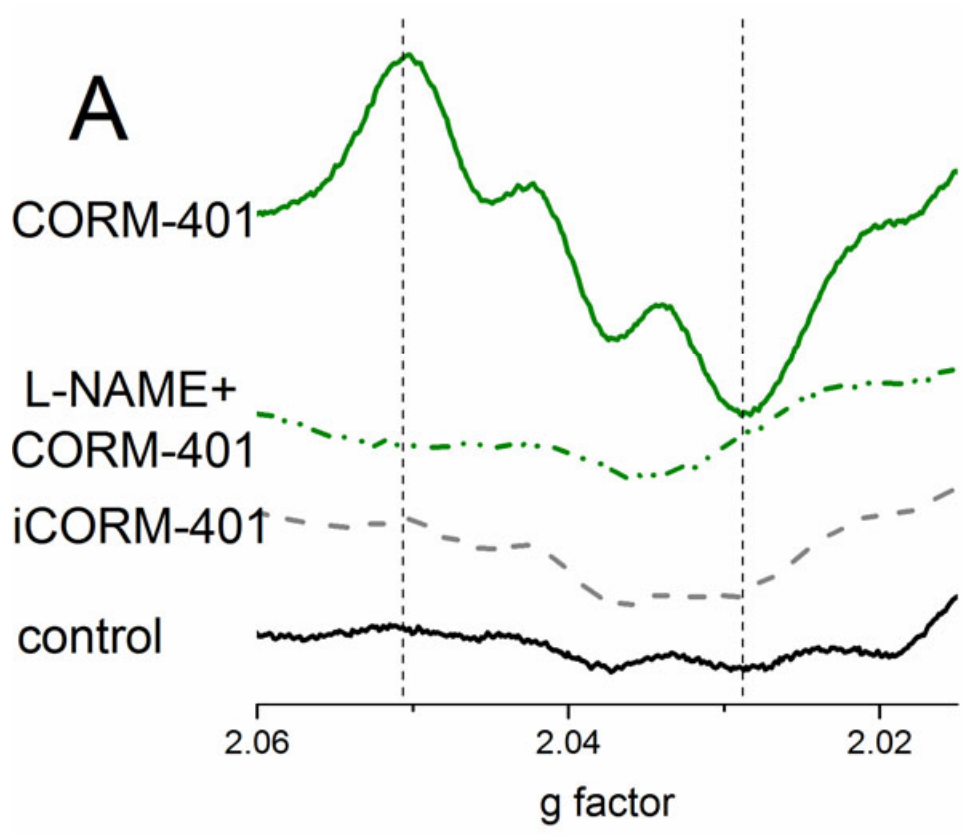
A

CORM-401

L-NAME+
CORM-401

iCORM-401

control

2.06   2.04   2.02

g factor

B

***   **

Fe(DETC)2-NO (AU)

100

75

50

25

0

control   CORM-401   iCORM-401
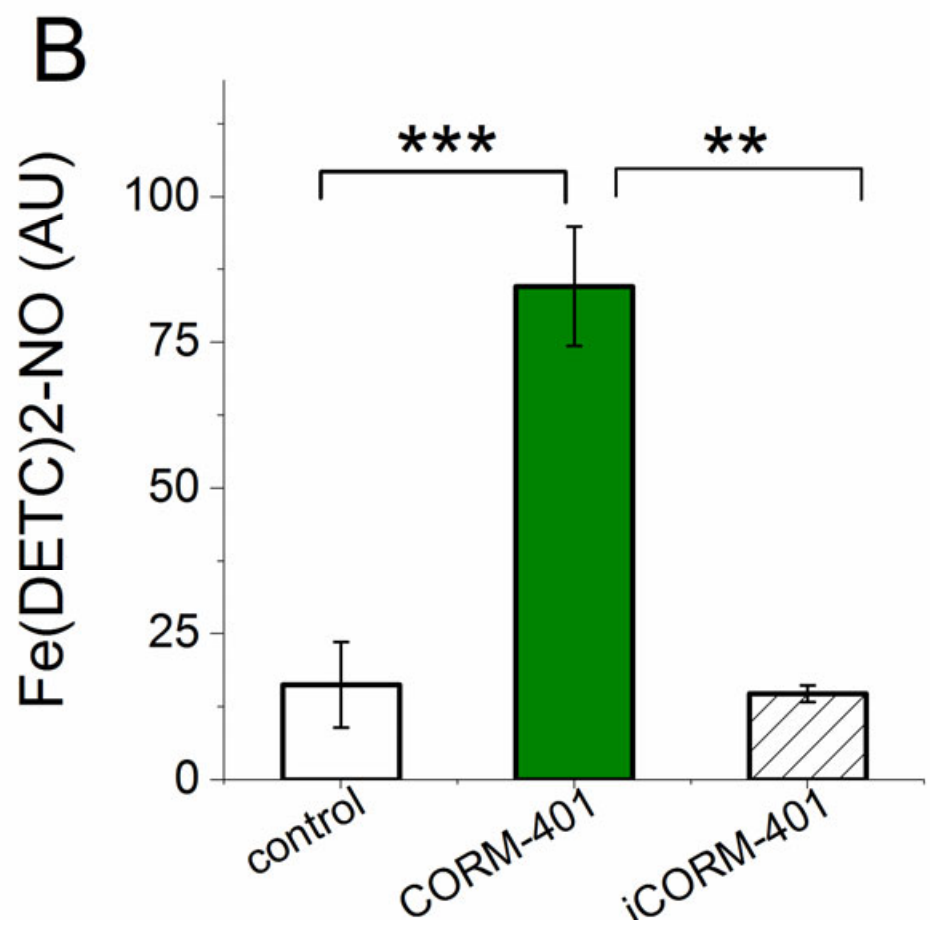
Figure 1

Carbon monoxide liberated from CORM-401 induces NO production in EA.hy926 endothelial cells. (A) Typical spectra for NO-$Fe^{2+}(DETC)_2$ adduct formed in EA.hy926 cells. (B) NO-$Fe^{2+}(DETC)_2$ adduct levels reflecting NO released by EA.hy926 cells untreated (control) or treated with 100 µM CORM-401 or 100 µM iCORM-401 (inactive compounds of CORM-401: ligand for CORM-401 + $MnSO_4$). Data are presented as mean ± SEM from three independent experiments, ** $P < 0.01$, *** $P < 0.005$.
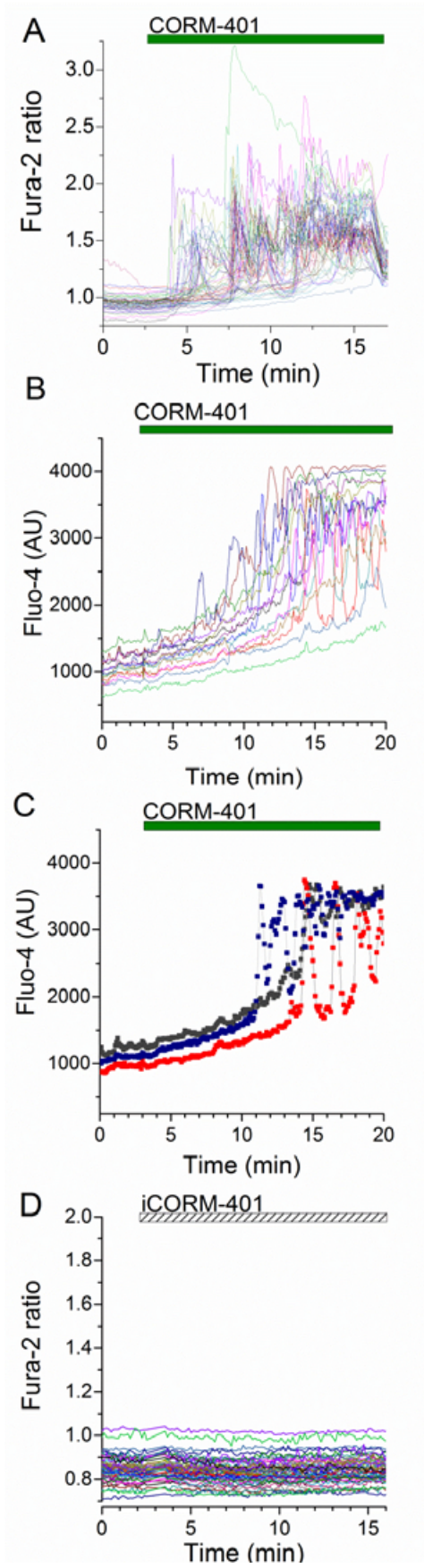
Figure 2

CORM-401 activates calcium signalling in EA.hy926 endothelial cells. Traces of Fura-2 (A, D) or Fluo-4 (B, C) fluorescence were recorded after addition of CORM-401 (A-C) or iCORM-401 (D). Sample traces (C) were extracted from the population presented in (B) to show different patterns of calcium signal: (1) gradually increasing calcium (reflecting global intracellular calcium concentration), (2) calcium peaks. A: n=14, D: n=55, E: n=147.
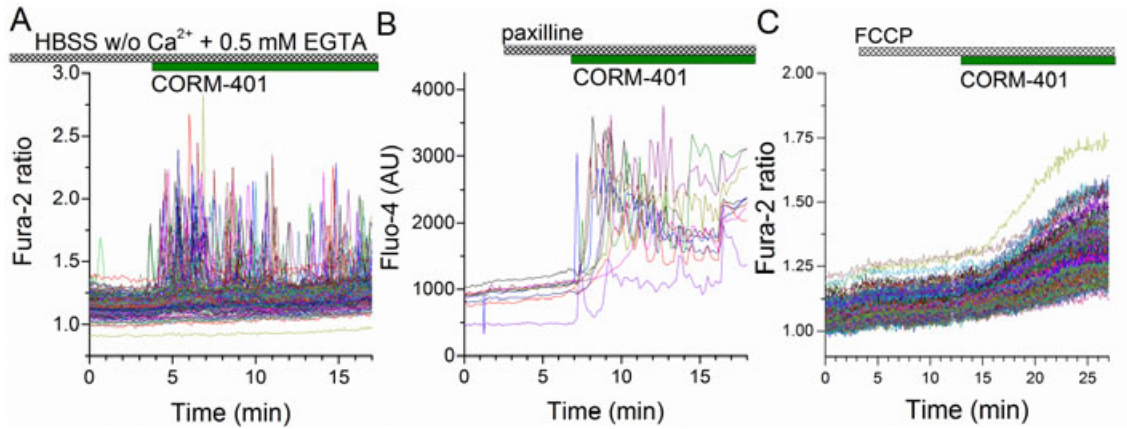
Figure 3

Cytosolic calcium signals induced by CORM-401 do not originate from extracellular calcium stores nor from mitochondria. Cytosolic Ca^{2+} signals stimulated by 30 μM CORM-401 in EA.hy926 cells (A) pre-incubated for 30 min in Ca^{2+}-free HBSS buffer containing 0.5 mM EGTA, (B) pre-treaded with 10 μM paxilline or (C) 0.5 μM FCCP. Each trace represents a single cell.
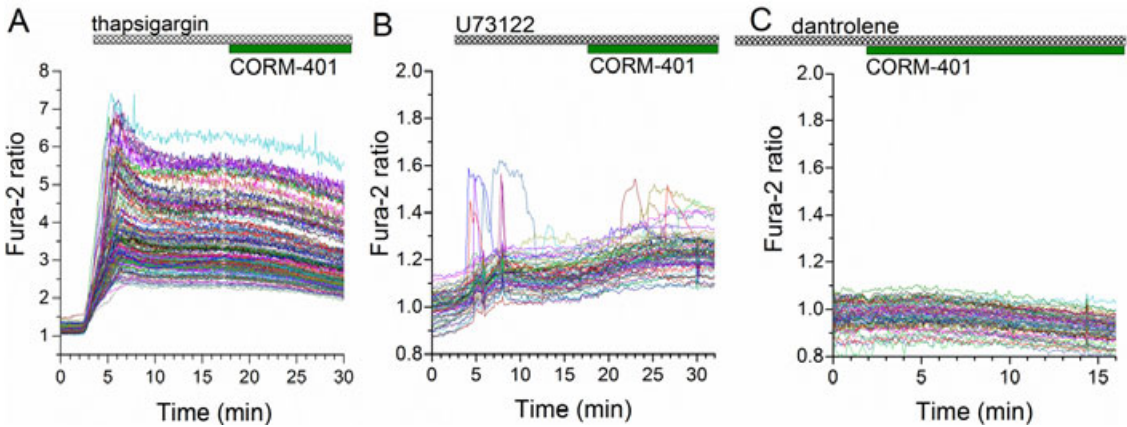

Figure 4

Cytosolic oscillatory calcium signals induced by CORM-401 are derived from endoplasmic reticulum (ER) through ryanodine receptors (RyR) activation. Cytosolic Ca^{2+} signals stimulated by 30 μM CORM-401 in EA.hy926 cells (A) pre-treated with 1 μM thapsigargin, (B) 5 μM U73122 or (C) 20 μM dantrolene. Each trace represents a single cell.
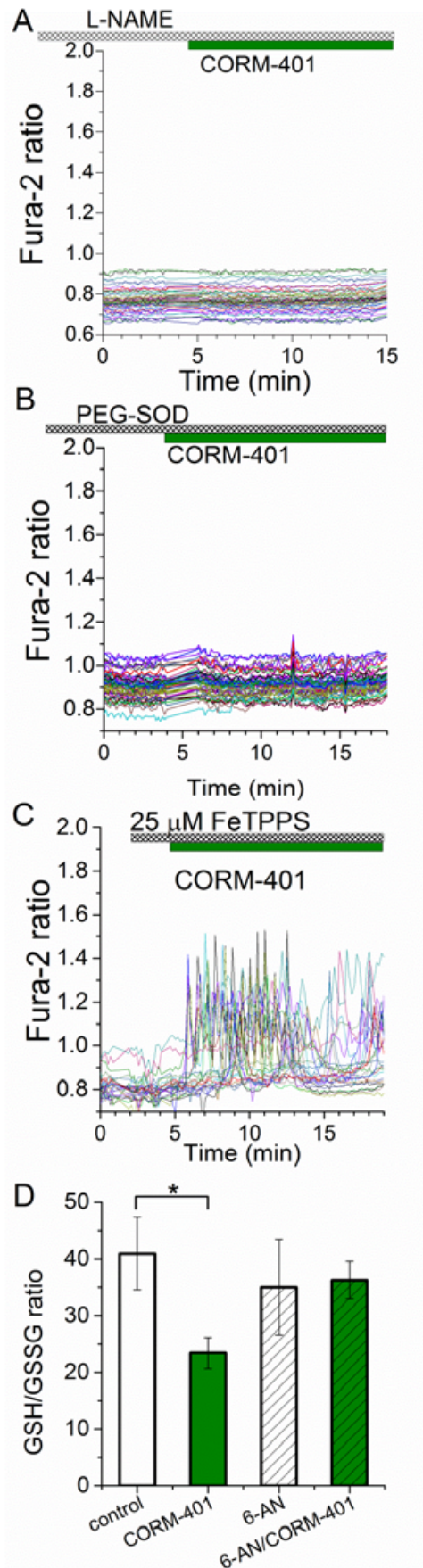
A

L-NAME

CORM-401

B

PEG-SOD

CORM-401

C

25 μM FeTPPS

CORM-401

D

Figure 5

NO and redox reactions mediate cytosolic calcium signals induced by CORM-401.
Cytosolic Ca^{2+} signals stimulated by 30 µM CORM-401 in EA.hy926 cells pre-treated with
100 µM L-NAME (A), 100 U/ml PEG-SOD (B) or 25 µM FeTPPS. Each trace represents a
single cell. (D) The ratio of reduced to oxidized glutathione (GSH/GSSG) in EA.hy926 cells
treated with 100 µM CORM-401 in response to 6-amononicotinamide (6-AN, 200 µM, pre-
incubation 4h); control cells were pre-incubated with DMSO as a vehicle (data are presented
as mean ± SEM from three independent experiments, * $P < 0.05$).
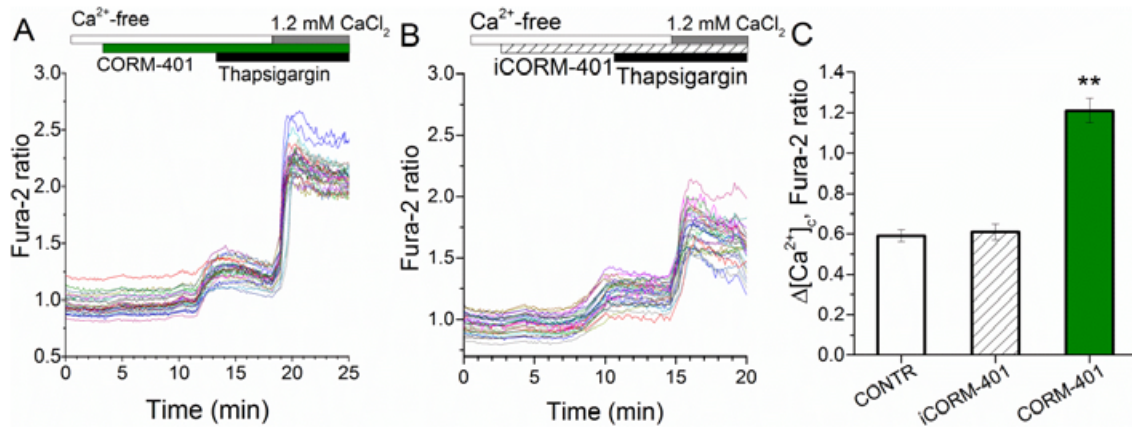
Figure 6

**Cytosolic slow and progressive calcium signals induced by CORM-401 are derived
from extracellular milieu through store-operated calcium (SOC) entrance.** Cytosolic
Ca^{2+} signals stimulated by 30 µM CORM-401 (A) or iCORM-401 (B) in EA.hy926 cells
placed in Ca^{2+}-free HBSS buffer followed by subsequent treatment with 1 µM thapsigargin
and restoration of Ca^{2+} ions. Each trace represents a single cell. (C) Changes in cytosolic
calcium concentrations in EA.hy926 cells untreated (CONTR) or treated with 30 µM iCORM-
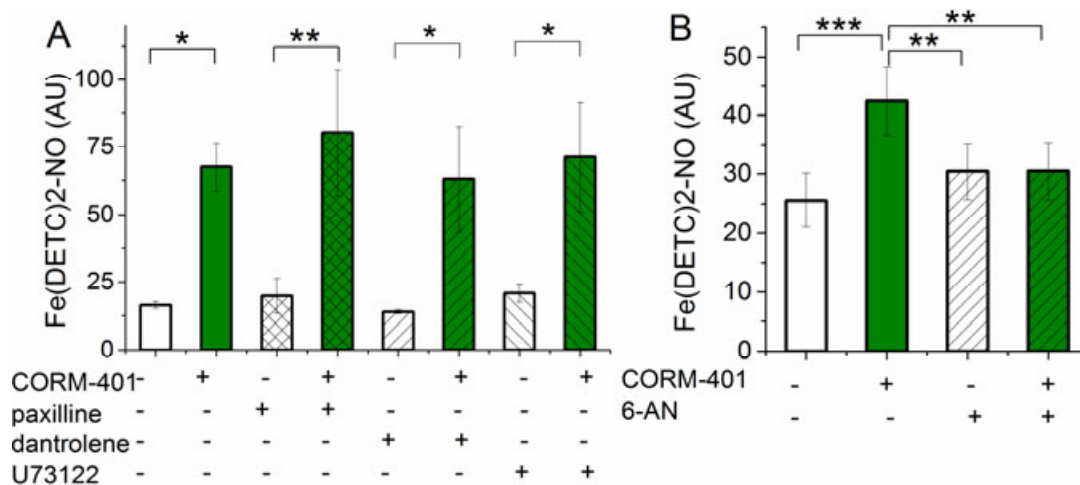401 or 30 µM iCORM-401 (data are presented as mean ± SD, ** $P < 0.01$).

Figure 7

CORM-401-induced NO production in EA.hy926 cells is supported by activation of the pentose phosphate pathway. NO-Fe^{2+}(DETC)$_2$ adduct levels reflecting NO released by EA.hy926 cells treated with 100 µM CORM-401 in response to (A) 10 µM paxilline, 5 µM dantrolene or 20 µM U73122, (B) 6-aminonicotinamide (6AN, 200 µM, pre-incubation 4h); control cells were pre-incubated with DMSO as a vehicle (data are presented as mean ± SEM from three independent experiments, ** $P < 0.01$, *** $P < 0.005$).
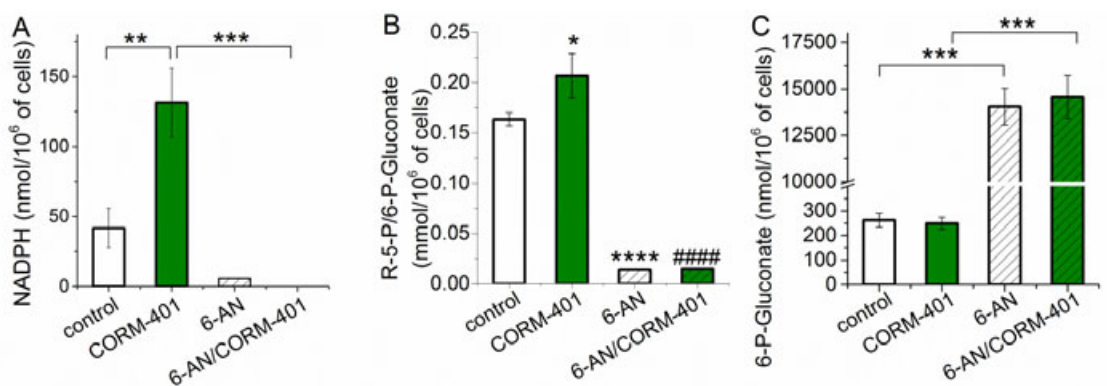
Figure 8

CORM-401 accelerates the pentose phosphate in EA.hy926 cells. (A) NADPH concentration, (B) the ratio of ribulose-5-phosphate (R5P) to its precursor 6-phosphogluconate (6PG) and (C) 6-P-Gluconate concentration in EA.hy926 cells treated with 100 µM CORM-401 in response to 6-amononicotinamide (6-AN, 200 µM, pre-incubation 4h); control cells were pre-incubated with DMSO as a vehicle (data are presented as mean ± SEM from three independent experiments, * $P < 0.05$, ** $P < 0.01$, *** $P < 0.005$, **** $P < 0.001$, #### $P < 0.001$; * as compared to untreated control, # as compared to CORM-401-treated group).